American Journal of Botany

Botanical Society of America
leading scientists and educators
since 1893

RESEARCH ARTICLE

Population genomics of a reindeer lichen species from North American lichen woodlands

Marta Alonso-García[1,2,6], Felix Grewe[3], Serge Payette[1], and Juan Carlos Villarreal A.[1,2,4,5]

Manuscript received 22 April 2020; revision accepted 28 September 2020.

[1] Département de Biologie, Université Laval, Québec G1V 0A6, Canada

[2] Institut de Biologie Intégrative et des Systèmes (IBIS), Université Laval, Québec G1V 0A6, Canada

[3] The Field Museum, Grainger Bioinformatics Center, 1400 South Lake Shore Drive, Chicago 60605, USA

[4] Royal Botanic Garden Edinburgh, 20A Inverleith Row, EH3 5LR, Scotland, UK

[5] Smithsonian Tropical Research Institute, Panama City, Panama

[6] Author for correspondence (e-mail: marta.alonso-garcia.1@ulaval.ca)

Citation: Alonso-García, M., F. Grewe, S. Payette, and J. C. Villarreal A. 2021. Population genomics of a reindeer lichen species from North American lichen woodlands. *American Journal of Botany* 108(1): 1–13.

doi:10.1002/ajb2.1601

PREMISE: Lichens are one of the main structural components of plant communities in the North American boreal biome. They play a pivotal role in lichen woodlands, a large ecosystem situated north of the closed-crown forest zone, and south of the forest–tundra zone. In Eastern Canada (Quebec), there is a remnant LW found 500 km south of its usual distribution range, in the *Parc National des Grands-Jardins*, originated mainly because of wildfires. We inferred the origin of the lichen *Cladonia stellaris* from this LW and assessed its genetic diversity in a postfire succession.

METHODS: We genotyped 122 individuals collected across a latitudinal gradient in Quebec. Using the software Stacks, we compared four different approaches of locus selection and single-nucleotide polymorphism calling. We identified the best fitting approach to investigate population structure and estimate genetic diversity of *C. stellaris*.

RESULTS: Populations in southern Quebec are not genetically different from those of northern LWs. The species consists of at least four phylogenetic lineages with elevated levels of genetic diversity and low co-ancestry. In *Parc National des Grands-Jardins*, we reported high values of genetic diversity not related with time since fire disturbance and low genetic differentiation among populations with different fire histories.

CONCLUSIONS: This first population genomic study of *C. stellaris* is an important step forward to understand the origin and biogeographic patterns of lichen woodlands in North America. Our findings also contribute to the understanding of the effect of postfire succession on the genetic structure of the species.

KEY WORDS Apothecia; *Cladonia stellaris*; dispersal; fire; population genomics; reproduction; Quebec; SNPs; Stacks.

The lichen woodland (LW) stands as the second largest ecosystem of the North American boreal biome, covering about 2 million km^2 in Canada, extending from the Atlantic coast to the Rocky Mountains and the Yukon (Johnson and Miyanishi, 1999; Payette and Delwaide, 2018). The LW is situated north of the closed-crown forest zone, and south of the forest-tundra zone (Fig. 1 from Payette et al., 2001). The ecosystem is an open forest with a characteristic continuous lichen ground cover (Girard et al., 2017) (Fig. 1A). Lichens are an important food source for reindeer (*Rangifer tarandus* L.) and caribou (*R. tarandus caribou*) in winter, accounting for 75% of their diet (Gauthier et al., 1989; Svihus and Holand, 2000). In Eastern Canada (Quebec), wildfires triggered the inception of LWs during the late Holocene (around 3000 BP) (Asselin and Payette, 2005). Since then, the frequency and intensity of fire events have increased resulting in the transformation of closed-crown boreal forest into LWs (Payette et al., 2000). The southernmost LWs in Canada, in the *Parc des Grands-Jardins* (PNGJ), were originated 1400 years ago (Jasinski and Payette, 2005) and they are found 500 km south of its usual distribution range (Fig. 2). The park is affected by three main disturbances: insect outbreaks, logging, and fires; the latter being the most significant. Around 120 km^2 of the PNGJ were burned by thirteen fires over the last century (Simard and Payette, 2001). The most recent fire occurred in 1999; before that, three remarkable fires happened in the 20th century (1991, 1940, and 1921), the oldest dating back to 1864 (Jasinski and Payette, 2005). These relatively recent disturbances make the park an ideal setting to explore fire effects on succession and composition changes of the southernmost LWs.

In the boreal biome, fire is the most significant disturbance (Payette, 1992; Bergeron et al., 2001; Lafleur et al., 2016) and it plays a major role in determining the distribution and composition of plant communities (Bergeron and Dubuc, 1989; Morneau and Payette,

FIGURE 1. Habitat and morphology of *Cladonia stellaris*. (A) Lichen woodland ecosystem in PNGJ. Dominance of black spruce (*Picea mariana* (Mill.) B.S.P.) and *Cladonia stellaris* covering the soil. (B) *Cladonia stellaris*. (C) Apothecia of *Cladonia stellaris* from *Alonso 428*.

1989; DeGrandpré et al., 1993; Kenkel et al., 1997). The successional fire stages in LWs of eastern Canada have been well documented (e.g., Ahti, 1959; Hustich, 1957; Kershaw and Rouse, 1976; Maikawa and Kershaw, 1976; Kershaw, 1978; Morneau and Payette, 1989; Webb, 1998; Héon et al., 2014; Girard et al., 2017). Based on changes in the abundance of lichen and moss species, four successional vegetation stages are generally identified (Ahti, 1961; Bergerud, 1971; Coxson and Marsh, 2001). During the first stage, crustose lichens such as *Trapeliopsis granulosa* (Hoffm.) Lumbsch and mosses (genus *Polytrichum* Hedw.) colonize the burned surface. Subsequently, the soil is covered by cup and horn lichens (*Cladonia cristatella* Tuck., *C. deformis* (L.) Hoffm., *C. crispata* (Ach.) Flotow, *C. sulphurina* (Michaux) Fr., etc.). The landscape remains mostly uniform for around 20 years until the arrival of fruticose *Cladonia* lichens. *Cladonia mitis* Sandst. and *C. rangiferina* (L.) F.H. Wigg. replace the previous lichen vegetation up to 60 years after fire (Morneau and Payette, 1989; Payette et al., 1989). *Cladonia stellaris* (Opiz) Pouzar & Vězda usually appears several decades after fire (Yarranton, 1975). Its abundance increases with time, and eventually, it becomes the dominant species forming extensive uniform carpets (Fig. 1A). In the absence of fire, *C. stellaris* woodlands can persist for centuries (Vézeau and Payette, 2016). Because of its abundance and persistence for years, this species is the most iconic example of mat-forming lichens present in LWs.

Cladonia stellaris (Fig. 1B) is broadly distributed in the Northern Hemisphere, mainly in boreal regions (Stenroos et al., 2018). Together with other reindeer lichens, it contains about 20% of the total LW biomass and can contribute up to 97% of ground cover (Auclair and Rencz, 1982; Morneau and Payette, 1989; Shaver and Chapin, 1991) because of its reproductive strategy. *Cladonia stellaris* reproduces mainly by fragmentation of the thallus (Yarranton, 1975). Apothecia (Fig. 1C), an indication of sexual reproduction, are considered either extremely rare (e.g., Vainio, 1897; Brodo et al., 2001; Athukorala et al., 2016) or overlooked (Ahti, 1961). In general, vegetative multiplication seems more prevalent than sexual reproduction in all reindeer lichens (Anderson and Rudolph, 1956; Bowler and Rundel, 1975). Vegetative propagules could be dispersed only tens of meters (Gauslaa, 1997; Heinken, 1999; Ronnås et al., 2017), whereas fungal spores can go through several hundred meters to kilometers (e.g., Heinken, 1999; Werth, 2010; Alors et al., 2017; Ronnås et al., 2017). Therefore, species that are predominantly asexual are expected to exhibit more genetic structure and low rates of gene flow (Werth, 2010; Grewe et al., 2018). Species reproducing predominantly asexually are also expected to have low values of genetic diversity (e.g., Seymour et al. 2005; Werth, 2010), with few genets (group of individuals genetically identical) in several to many ramets (each individual from a genet) (Yarranton, 1975). In addition, genetic diversity of some clonal lichens seems to depend on environmental disturbance, being lower in burned areas (Werth et al., 2006).

Based on the life history traits of the species, we ask two questions: Are the populations of *C. stellaris* from southern Quebec isolated from those in northern LWs? How did the fire affect the genetic diversity of *C. stellaris* in the PNGJ? To answer them, we explore the population structure of this lichen and the potential link between fire disturbances and genetic diversity. Our specific objectives are to (1) infer the origin of *C. stellaris* from the southernmost LWs of the PNGJ, and (2) correlate its genetic diversity with successional post-fire stages in the PNGJ. To achieve these objectives, we analyzed genotype-by-sequencing data as was successfully done for lichens before (Grewe et al., 2017). We compared four different approaches of locus selection and single-nucleotide polymorphism (SNP) calling and identified the best fitting approach to investigate population structure and estimate genetic diversity of the lichen *C. stellaris*.

MATERIALS AND METHODS

Sampling

A total of 122 individuals of *C. stellaris* were sampled across a latitudinal gradient in Quebec (subcontinental scale), with six samples

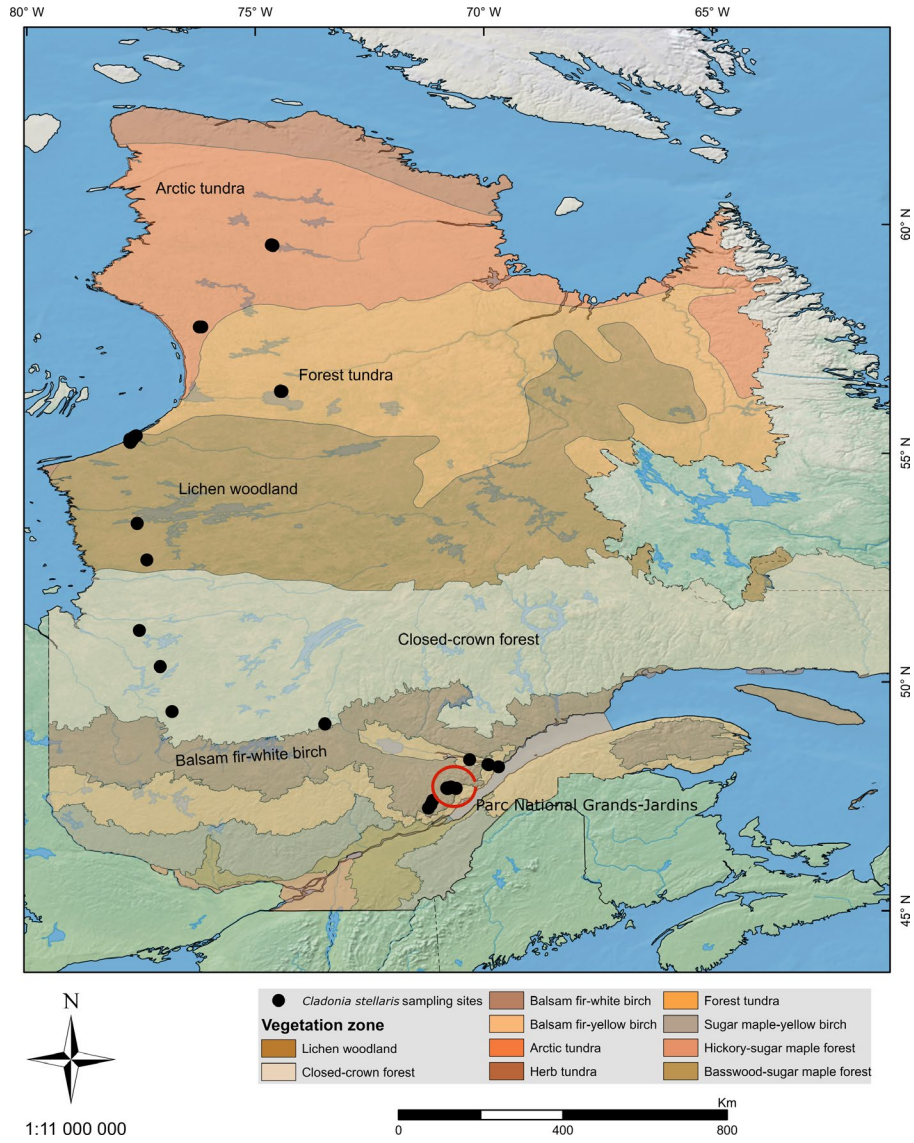

FIGURE 2. Map of sampling locations of *Cladonia stellaris* across a latitudinal gradient in Eastern Canada. The different vegetation zones are highlighted, and black circles show the sampling sites.

from arctic tundra, three from forest tundra, 22 from northern LWs, 72 from the LWs of the PNGJ, and 19 from closed-crown forests (Fig. 2; Appendix S1, Table S1).

The more intensive sampling at the PNGJ (landscape scale) corresponded to burned sites in 1999, 1991, 1940, 1921, and 1864. The maximum and minimum distances between sites were 10 and 1 km. At each site, 10–30 individuals were randomly sampled. The minimum distance between individuals within site was 10 m. In the 1999 site, we only found two patches of *C. stellaris*. Individuals of *C. mitis* were also collected to compare the data at the species level (five samples from site 1999 and three samples from 1991) (Appendix S1, Table S1).

In *C. stellaris*, podetia (vegetative thallus) form compact subglobose heads growing singly in groups or in mats (Fig. 1B). Here, we consider each of those heads a different individual. In *C. mitis*, single-branched podetia were used. Fragments of a single individual were placed into an Eppendorf tube, airdried for 24 h, then stored at –20°C. Herbarium vouchers were deposited in the Louis-Marie Herbarium (herbarium code QFA), Laval University.

Library preparation and sequencing

DNA was extracted following an already published protocol (Park et al., 2014). A double-digest genotyping-by-sequencing (GBS) library (enzymes PstI/MspI) was prepared for Ion Torrent sequencing (as per Mascher et al., 2013). Single-end sequencing was performed on an ion proton machine at the *Plateforme d'analyses génomiques* (*Institut de Biologie Intégrative et des Systèmes*), at Laval University (Quebec City, QC, Canada). Ion proton technology offers greater speed and an almost absence of discordance (1–2%) with Illumina technology when using the same SNP calling pipeline (Mascher et al., 2013). A total of 204 million reads (25–235 bp) were obtained (Appendix S1, Table S2).

Quality control and demultiplexing reads

Demultiplexing, filtering, and trimming were executed using the pipeline *process-radtags* of Stacks v2.3 (Rochette et al., 2019) (Fig. 3). Parameter settings are provided in Appendix S2. We first demultiplexed reads of individuals from the pool of raw sequence reads based on their barcodes. Then, we filtered the reads based on the quality value of a base using Phred+33 encoding. To make the reads' length uniform, we checked the sequence length distribution from FastQC v0.11.3 (Andrews, 2010) and trimmed all reads to 125 base pairs.

Generating genomic data sets

Map to a reference—We used five publicly available genomes and transcriptomes of species of the genus *Cladonia* as references, such as the complete genomes of *C. grayi* (Armaleo et al., 2019), *C. macilenta* (GenBank accession AUPP00000000), *C. metacorallifera* (GenBank accession AXCT02000000) and *C. uncialis* (BioProject accession PRJNA348097), and the transcriptome of *C. rangiferina* (BioProject accession PRJNA147995). We first mapped our reads to each single genome. However, to increase the number of reads mapped, we merged the four genomes and the transcriptome into a single file, and we used it as reference.

Cleaned reads from *process-radtags* for each sample were aligned to the reference using two different software packages, bowtie2 v2.3 (Langmead and Salzberg, 2012) and bwa v0.7 (Li and Durbin, 2009) (Fig. 3). For bowtie2, we selected the more accurate option (*--very-sensitive*) and *--end-to-end* mode (Appendix S2), that is, alignments involving all of the read characters. By contrast,

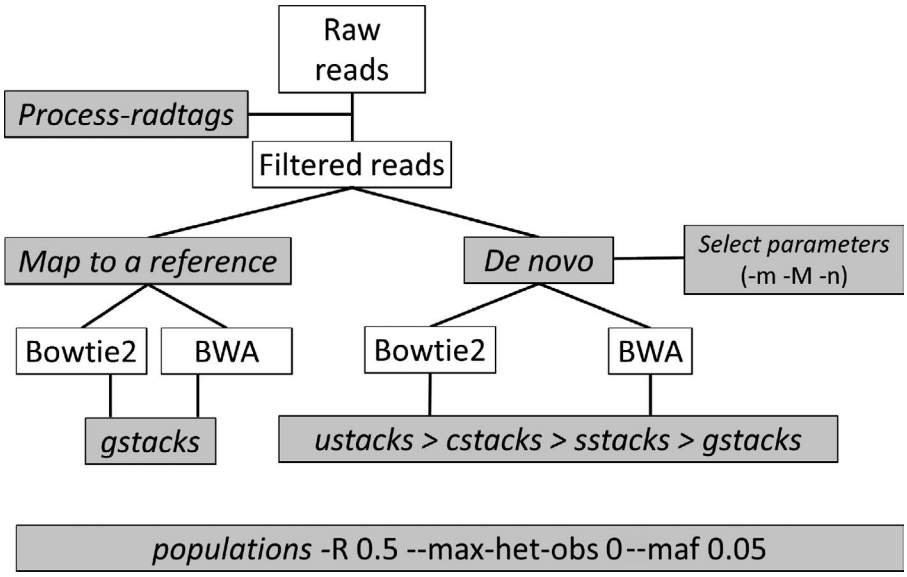

FIGURE 3. Overview of the genotype-by-sequencing (GBS) data processing flowchart.

in a local alignment, some reads characters are trimmed from the ends of the alignment. The bwa package was configured as *mem* (Appendix S2) because the algorithm is robust to sequencing errors and applicable to long sequence lengths (>70 bp). Moreover, it automatically chooses between end-to-end and local alignments (Li, 2013). With the Samtools suite, we converted the outputs of bowtie2 and bwa (SAM format) to the equivalent compressed BAM format as suggested by Rochette and Catchen (2017).

De novo assembling—*Select optimal parameters*—To identify the optimal parameters for assembling loci in Stacks, we followed the parameter-testing pipeline established by Rochette and Catchen (2017) and Paris et al. (2017). We first selected a subset of 10 representative samples (popmap denovo test, Appendix S1, Table S1), based on the read coverage numbers obtained with *process-radtags* and the expected genetic similarities among samples (individuals from the same sampling locality). We ran the Stacks pipeline on this subset to investigate a range of parameter values (Paris et al., 2017; Rochette and Catchen, 2017). The *-M* parameter is the maximum distance in nucleotides allowed between stacks, *-m* is the minimum depth of coverage required to create a stack, and *-n* is the number of mismatches allowed between loci when building the catalog. We increased *-M* from 1–6 (fixing M = n) while keeping *-m* constant at 3. We identified the minimum value of *-M* that maximized the number of recovered loci. The number of variant sites remained almost constant through all *-M* values, being slightly higher for *-M 6*. We selected 2 as the optimal value for *-M*. We then held *-M* constant at 2, and iteratively varied the *-n* parameter to determine whether this resulted in an appreciable difference on the number or recovered loci and variant sites (Spalink et al., 2019) (Appendix S2). The results showed a substantial difference for *-n 1* and *-n 6*, while *-n 2*, *-n 3*, *-n 4*, and *-n 5* generated very similar results. We used a similar approach for a constant value of *-n* 2, varying *-M* value. Finally, we concluded that the suitable value to our data set corresponds to 2 for *-M* and *-n*.

Run Stacks de novo—Two different data sets were used as input: (1) reads aligned to the reference genomes with bowtie2, and (2) reads aligned to the references with bwa (Fig. 3), so that we were processing only *Cladonia* mycobiont reads. For the bwa data set, *process-radtags* had to be run a second time to homogenize read length.

The Stacks pipeline was run with considering each individual a single population (popmap individuals, Appendix S1, Table S1) to obtain genetic data for each individual (number of loci, coverage, and number of genotypes). The parameters were as follows: *ustacks* (*-m 3 -M 2 -H*), *cstacks* (*-n 2*), *sstacks*, *tsv2bam*, and *gstacks* (default parameters: *--model marukilow* and *--var-alpha 0.05*). The fungal partner of the lichen is haploid and thus, the *-H* option was selected (Pan et al., 2015). The last step, *gstacks*, created the loci for our samples (Fig. 3).

Reference-based analysis—To perform the map-to-reference analysis, we aligned reads to our merged reference genomes and used mapping information as guidance to build sequence stacks. We ran the pipeline on both data sets: bowtie2 and bwa. The *gstacks* option (Stacks pipeline) was run with default parameters (*--model marukilow* and *--var-alpha 0.05*) considering each individual a single population (popmap individuals, Appendix S1, Table S1), to create loci (Fig. 3).

SNPs calling using outputs from different approaches—The SNPs were called by the four approaches (bowtie2-mapping, bwa-mapping, bowtie2-denovo, and bwa-denovo), that is, we used as input for the analysis the four sets of output (loci) derived from *gstacks* (Fig. 3). The *population* module was run considering each individual a single population (popmap individuals, Appendix S1, Table S1). On the first call, loci present in at least 50% (*-R 0.5*) of the individuals were kept. Unshared SNPs were pruned to reduce haplotype-wise missing data (with *--filter-haplotype-wise*). Maximum observed heterozygosity was set up at 0 (*--max-obs-het 0*) and the minimum minor allele frequency (MAF) at 0.05 (*--min-maf 0.05*) (Fig. 3). Table 1 shows the total number of loci and SNPs of *C. stellaris*, for each approach, before and after filtering using populations (Stacks). De novo approaches generated many more loci than the mapping approaches (Table 1). However, once we retained just loci that occurred at certain frequencies (postfilter), the two mapping approaches provided more loci. We obtained 275 and 1450 SNPs from bowtie2-mapping and bwa-mapping, respectively (Table 1).

Based on these results, we selected bwa-mapping approach to infer the population structure of *C. stellaris* in Quebec (subcontinental scale) and to estimate genetic diversity in a postfire succession within the PNGJ (landscape scale). Results inferred from bowtie2-mapping are detailed in the Supplementary Information.

Inferring population structure at a subcontinental scale

Identification of genetic clusters—To identify the genetic groups of *C. stellaris* in Quebec, a maximum likelihood (ML) phylogenetic analysis and a principal component analysis (PCA) were performed. A total of 724 unlinked SNPs (Table 1) were used for the phylogenetic analyses. A ML phylogeny was performed using RAxML v8.2.9 (Stamatakis,

TABLE 1. Total number of loci and SNPs detected for 122 samples of *Cladonia stellaris* using four different bioinformatic approaches with the Stacks software package.

Approach	bowtie2-mapping	bwa-mapping	bowtie2-denovo	bwa-denovo
No. loci prefilter	10752	28046	211300	370070
No. loci postfilter (-R 0.5)	659	2017	14	20
No. variant sites postfilter (-R 0.5)	275	1450	1	12
No. unlinked variant sites postfilter (-R 0.5)	171	724	1	11

2014) with a *GTRGAMMA* model. For the analysis, 100 bootstrap replicates were calculated using the fast bootstrapping option (*-f a*). We used a function for SNP data sets that correct the likelihood for ascertainment bias-associated error (*-m ASC_GTRGAMMA --asc-corr=lewis*) (Stamatakis, 2014) (Appendix S2).

The bwa-mapping data set was converted to *genind* and *genlight* objects using the R package Adegenet v 2.0.2 (Jombart et al., 2016). Missing data were calculated (Appendix S2) and a PCA was carried out.

Estimation of genetic diversity—To determine genetic diversity of *C. stellaris*, we classified our samples according to the results from the ML analysis (Fig. 4) (Popmaps RAxML, Appendix S1, Table S1). The summary statistics for the phylogenetic clusters were calculated in Stacks. A second SNP call was run using a population map based on the phylogenetic clades (Popmaps RAxML, Appendix S1, Table S1). A total of five populations were designated, each population corresponds with one clade from the ML tree (Fig. 4), such as clade A, clade B, clade C, clade D, or clade E (unsupported clade). A stronger filter was applied so that at least 75% of individuals in a population (within each clade) must share a locus to process it for that population (*-r* 0.75). Maximum observed heterozygosity and minimum minor allele frequency were set up as previously (*--max-obs-het 0 --min-maf 0.05*); *--filter-haplotype-wise* and *--fstat* options were included to reduce missing data and estimate pairwise fixation index (*Fst* values), respectively. The maximum *p*-value to keep a *Fst* measurement was set up at 0.05.

Calculation of the co-ancestry matrix—The population genetic structure of *C. stellaris* at a subcontinental scale was also assessed using a Bayesian model-based approach with the program fineRADstructure (Malinsky et al., 2018). The software recovers the nearest-neighbor haplotype relationships and it is specifically designed to measure population structure amongst haplotypes inferred from RADseq data sets. We first converted the haplotype output from populations (Stacks) to a fineRADpainter input file,

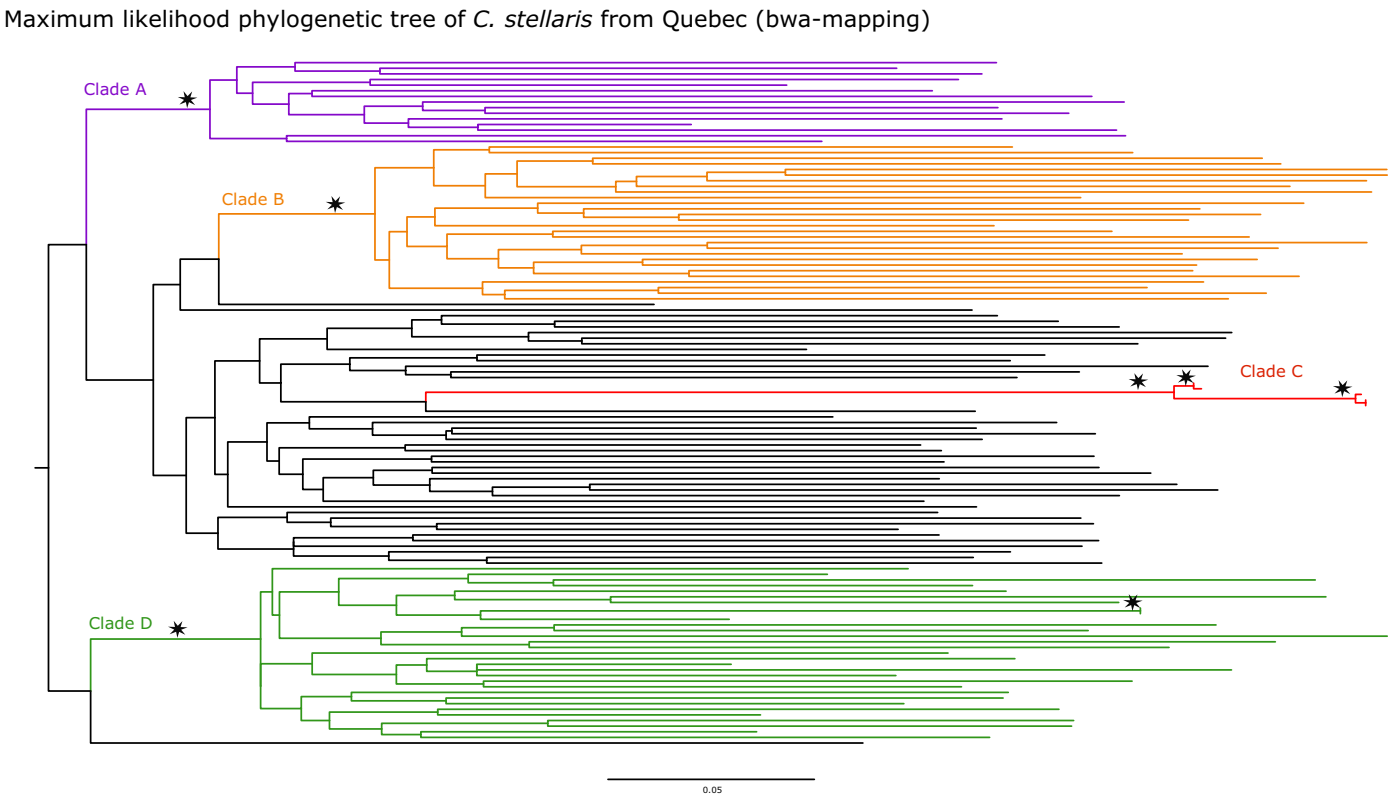

FIGURE 4. Maximum likelihood phylogenetic tree inferred from *Cladonia stellaris* GBS data. Tree was built from 724 unlinked SNPs data set from bwa-mapping approach and midpoint rooted. Well-supported branches (Bootstrap values >90) are marked with a start.

reducing the maximum number of SNPs allowed at a locus to 10 (http://cichlid.gurdon.cam.ac.uk/fineRADstructure.html). We reordered the loci with the script provided (*sampleLD.R*). Afterwards, the co-ancestry matrix (*RADpainter*) was estimated, the individuals were assigned to populations, and the coalescence tree was built (*finestructure*) (Appendix S2). The output was loaded into the program finestructure GUI for visualization.

Assessing genetic diversity at landscape scale

We included the 72 samples of *C. stellaris* collected in the park. We also added eight samples of *C. mitis* from the 1991 and 1999 fire sites. Based on reads previously mapped to the reference using the bwa-mapping approach, *gstacks* created the loci with default parameters and considering each individual a single population. To call SNPs, individuals were grouped by species (Popmap PNGJ species, Appendix S1, Table S1). Loci shared by at least 75% (*-r* 0.75) of the individuals within each species were kept. The same filters as before were applied (*--filter-haplotype-wise --max-obs-het 0 --min-maf 0.05*). A PCA was performed and the pairwise *Fst* values calculated with *p*-values describing if the *Fst* measures were statistically significant according to Fisher's Exact Test. We also applied a second filter to the data to investigate genetic diversity within fire events and to compare *Fst* values. In this case, samples were grouped not only by species but also by fire event (Popmap PNGJ species and fire, Appendix S1, Table S1). Because of the Stacks fixed setting, each species could be assigned only to one fire event, hence, we included specimens of *C. mitis* from 1999 and those of *C. stellaris* from 1991, 1940, 1921, and 1864. A PCA was performed and the pairwise *Fst* values were calculated.

RESULTS

Variant calling with four approaches

Genotyping-by-sequencing and mapping to a reference—Approximately 204 million sequencing reads were generated for 122 samples of *C. stellaris*. The total number of reads retained after demultiplexing, filtering, and trimming were ~158 million varying from 104,333 for sample Alonso_505 to 8,738,319 for Alonso_604 (Appendix S1, Table S2).

After mapping to the fungal references to filter out nonfungal sequences, the number of reads was drastically reduced. The bowtie2 package retained an average of 0.30% of reads, and bwa an average of 0.40%. A comparison of the total number of reads can be found in Appendix S1, Table S3. In general, the number of reads kept for each sample differed slightly between the two mapping programs but was always higher for bwa.

gstacks results for de novo and mapping approaches—The total number of loci of *C. stellaris* before filtering (*gstacks*) was higher for the de novo approaches than for the mapping. Appendix S1, Table S4 compiles detailed *gstacks* results for the four approaches and it shows the number of loci and mean depth coverage for each sample and each approach. The two de novo approaches (bowtie2 and bwa) recovered more loci (mean number of 3793 and 5935, respectively), but the samples had the lowest depth coverage (37X and 27X, respectively). By contrast, the mean number of loci for the mapping approaches was lower (919 for bowtie2 and 2925 for bwa) and they presented higher depth coverage (47X and 85X mean, respectively).

SNPs called for each approach—Results of the populations module (SNPs calling) are detailed in Appendix S1, Table S5. The table compares the number of private, variant, and polymorphic sites (SNPs) for each sample and approach. To have statistics results for each individual, they were treated as independent populations (Popmaps individuals, Appendix S1, Table S1). Private sites are the alleles unique to each individual, variant sites are those that vary across all individuals, and polymorphic sites (SNPs) are those variants inside each individual. The de novo approaches detected a small number of variant sites (mean number of 0.5 and 6.7 for bowtie2-denovo and bwa-denovo, respectively), whereas the mapping approaches called a mean number of ~200 and 1000 variant sites, respectively (Appendix S1, Table S5).

Population structure at a subcontinental scale using bwa-mapping approach

***Genetic clusters of* C. stellaris**—The proportion of missing data in the phylogenetic analysis was 23%. We used a midpoint rooting for the phylogenetic tree and considered a supported clade as a group of individuals clustered together with a bootstrap value (BS) ≥90 (Fig. 4). Four main clades were recovered: clade A, clade B, clade C, and clade D. The main difference between bowtie2-mapping and bwa-mapping approaches was found in the position of five samples from the 1940 fire in PNGJ (Alonso 608, 609, 610, 611, and 612) (popmaps RAxML, Appendix S1, Table S1). Using bowtie2-approach (Appendix S3), they were split in two different supported clades (BS = 100) (Alonso 608 and 610; Alonso 609, Alonso 610, and Alonso 611), with the second one located inside clade B.

The first two principal component axes explained 46.1% and 29.42% of variance in bwa-mapping (Fig. 5). In the plotted PCA, all individuals from clade C (1940 fire, PNGJ) fell out of the central cloud as outliers (Fig. 5). The percentages of missing data calculated with the package Adegenet are listed in Appendix S1, Table S6; the

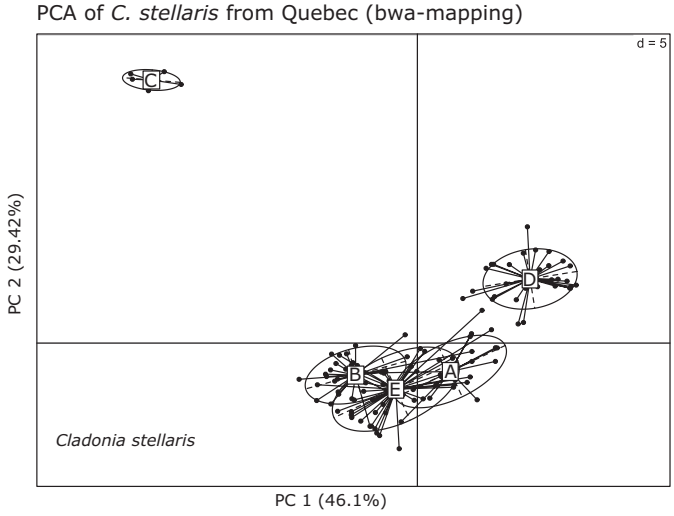

FIGURE 5. PCA of *Cladonia stellaris* in Quebec using 1450 SNPs from bwa-mapping approach. Letters corresponds with maximum likelihood phylogenetic clades (Fig. 4).

TABLE 2. Summary population statistics for the phylogenetic clades of *Cladonia stellaris* in Quebec. Results derived from the bwa-mapping approach and filtered with *-r 0.75 --max-obs-het 0 --min-maf 0.05*. All positions (variant and fixed) are shown. Statistics include Num ind. (total average number of individuals genotyped at each locus), private sites (number of unique sites to each population), sites (total number of sites for each population), variant sites (number of sites across all populations that are variant), % variant (percentage of variant sites), polymorphic sites (SNPs) (number of sites inside each population that are variant), PPS% (percentage of polymorphic sites), and π (mean nucleotide diversity).

bwa-mapping # All positions (variant and fixed)								
Phylogenetic clades	**Num Ind**	**Private**	**Sites**	**Variant**	**% Variant**	**Polymorphic**	**% PPS**	**π**
A	14.2	73	173769	781	0.45	561	0.32	0.00090
B	26.0	196	198520	1054	0.53	914	0.46	0.00125
C	4.8	20	278762	1075	0.39	103	0.04	0.00019
D	28.9	33	168009	720	0.43	597	0.36	0.00082
E	39.7	50	173648	791	0.46	718	0.41	0.00099

highest value was 54% and the lowest was 5%. PCA derived from bowtie2-mapping approach is shown in Appendix S4.

Genetic diversity within and among phylogenetic clusters—The bwa-mapping data set generated 28046 loci and 25583 were not kept. The 2463 loci kept had 311348 sites and 1293 SNPs. Table 2 includes values of genetic diversity after filtering. The number of variant sites was usually slightly higher than the number of SNPs, except for clade C. The mean percentages of variant sites and SNPs were 0.45% and 0.32%, respectively. Clades C (five samples from the 1940 fire) and B had more variant sites (1075 and 1054, respectively) than the other clades (Table 2). The greatest numbers of SNPs and private sites were also found in clade B (914 SNPs and 196 private sites). By contrast, clade C presented the lowest number of SNPs (103) (Table 2). The nucleotide diversity (π) was always more diverse in clade B (0.00125), and less diverse in clade C (0.00019) (Table 2). When just the variant position, i.e., not fixed and variant, were included, the values (not shown) of nucleotide diversity were higher (mean π of 0.18). Using the bowtie2-mapping data set, 9871 loci from 10752 did not pass the population filter (*-r 0.75 --max-obs-het 0 --min-maf 0.05*). A total of 881 loci were kept, composed of 111594 sites; 233 of those sites were SNPs. The summary population statistics are detailed in Appendix S1, Table S7.

Pairwise *Fst* values comparisons between clades ranged from 0.03–0.22 (Appendix S1, Table S8). The clades A–C exhibited the highest *Fst* values (*Fst* = 0.22), followed by clades C–D (*Fst* = 0.18), B–C (*Fst* = 0.13) and C–E (*Fst* = 0.11). The remaining pairwise comparisons showed *Fst* values lower than below 0.10 (Appendix S1, Table S8). Pairwise *Fst* comparisons for the bowtie2-mapping approach are also detailed in Appendix S1, Table S8.

Co-ancestry matrix—The analyses performed with fineRADstructure provided additional information about ancestry between individuals of *C. stellaris* from Quebec (Fig. 6). It revealed a pattern consistent with our previous results, with the exception of sample Alonso_374. It was included in clade A in ML analysis (Fig. 4) but grouped within the unsupported clade (E) in the co-ancestry analysis (fineRADstructure) (fineRAD results, Appendix S1, Table S1) (Fig. 6). The analyses generated five clusters where individuals share more co-ancestry with each other than between clusters. The highest co-ancestry was found in clade C, followed by clades A, D, B, and E (Fig. 6). The co-ancestry matrix derived from the bowtie2-mapping approach can be found in Appendix S5.

Genetic diversity at a landscape scale using bwa-mapping approach

Summary statistics in a postfire succession—We tested the correlation between genetic diversity of *C. stellaris* in PNGJ and the successional fire stages. We first calculated genetic diversity of two species (*C. stellaris* and *C. mitis*) to have an overall idea of the diversity of the reindeer lichens within the park; then we assessed the differences among postfire stages. A total of 3205 loci and 5329 SNPs were retained. *Cladonia stellaris* had fewer SNPs (1581) than *C. mitis* (3627) (Appendix S1, Table S9A). Nevertheless, the former exhibited a large number of exclusive alleles (private sites) (408 vs. 145) (Appendix S1, Table S9A). Results from bowtie2-mapping are detailed in Appendix S1, Table S9B.

The first two PC axes explained 76.54% and 14.03% of variance, respectively (Appendix S6A). The PCA plotted three separate clusters, *C. stellaris*, *C. mitis*, and clade C from the ML analysis (five samples of the 1940 fire). The *Fst* value between *C. stellaris* and *C. mitis* was 0.41. PCA results for bowtie2-mapping are presented in Appendix S6B.

The second filter allowed us to test the correlation of genetic diversity and time from the last fire event. Table 3 shows summary statistics for each stage (1999, 1991, 1921, 1940, and 1864). The number SNPs of *C. stellaris* throughout the succession stages varied between ~1500 SNPs in the older sites (1864 and 1921 fire) and 1904 SNPs in 1940 fire (Table 3). The number of private sites ranged from 26 (1864 fire) to 94 (1940 fire). Summary statistics throughout the succession inferred from bowtie2-mapping approach can be found in Appendix S1, Table S10.

In the PCA (Fig. 7), most of the variance was explained by the first two PC axes (65.92% and 22.76%, respectively). *Cladonia mitis* (1999 fire) and *C. stellaris* (fires 1991, 1940, 1921, and 1864) were clearly separated (Fig. 7). Individuals of *C. stellaris* from site 1991 and 1940 grouped closer among them than to those from 1864 and 1921. In addition, the five individuals of clade C clustered together, excluding the remaining samples from the 1940 fire (Fig. 7). The *Fst* values between *C. mitis* and populations of *C. stellaris* were over 0.75. Among fire sites, *Fst* values were lower than 0.06 (Appendix S1, Table S11). Plotted PCA and *Fst* values from the bowtie2-mapping approach are shown in Appendix S7 and Table S11 in Appendix S1, respectively.

DISCUSSION

This first population genomic study of the emblematic reindeer lichen *C. stellaris* elucidates the origin of the southern Quebec populations

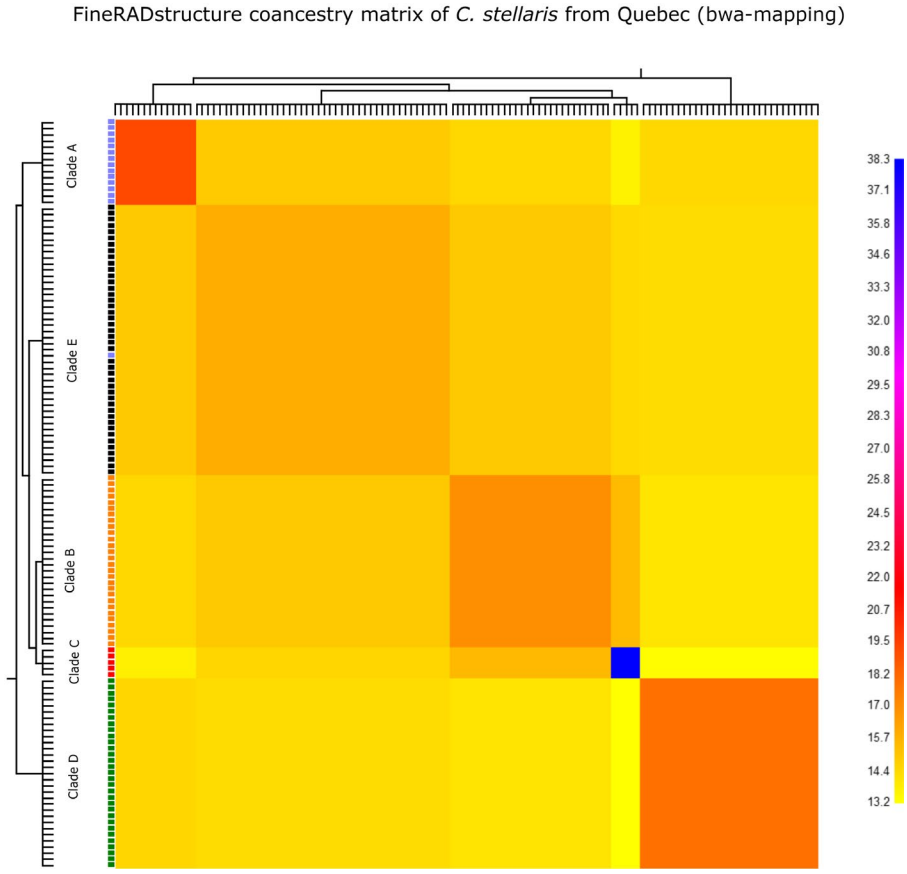

FIGURE 6. Clustered fineRADstructure co-ancestry matrix of *Cladonia stellaris* in Quebec estimated from 724 unlinked SNPs from bwa-mapping approach. The heatmap shows pairwise co-ancestry between individuals, with blue representing the highest level, red and orange indicating intermediate levels, and yellow representing the lowest levels of shared co-ancestry. The names of clades follow those of maximum likelihood tree (Fig. 4).

and assesses the correlation between genetic diversity and successional postfire stages. We analyzed the data using four different approaches and selected the best to conduct a population genomic analysis. We found no evidence of spatial genetic structure of *C. stellaris* throughout the Quebec region. The species consists in, at least, four phylogenetic lineages with elevated levels of genetic diversity and low co-ancestry. At a landscape scale (PNGJ), we reported high values of genetic diversity not related with time elapsed since the last fire disturbance, and low genetic differentiation between fire sites.

Lack of spatial structure at a subcontinental scale

Several authors have suggested the absence of sexual reproduction in reindeer lichen *Cladonia* species (e.g., Vainio, 1897; Anderson and Rudolph, 1956) and highlighted the importance of multiplication by fragmentation (e.g., Bowler and Rundel 1975; Yarranton, 1975; Webb, 1998). Clonal propagules in lichens are usually dispersed only in tens of meters (e.g., Gauslaa, 1997; Heinken, 1999; Ronnås et al., 2017). Thus, we expected a geographic and genetic structure of southern Quebec populations, similar to that reported in the clonal Northern Hemisphere lichen *Lobaria pulmonaria* (L.) Hoffm. (Werth et al., 2007). However, our results reflect lack of spatial structure and unrestricted migration within the region. Walser et al. (2005) investigated the population structure of three Swiss populations of *L. pulmonaria*, with a high degree of vegetative propagation, and they also found no differentiation among populations at a similar scale. Likewise, Degtjarenko et al. (2018) showed unconstrained gene flow between populations of the mainly clonally reproducing *Usnea subfloridana* Stirt. A possible explanation to our results would be that long-distance dispersal (LDD) e.g., of thallus fragments, actually occurs in *C. stellaris*. The study of Werth et al. (2006) showed that dispersal of clonal propagules over larger distances (i.e., >200 m) may be a rather common phenomenon in other lichens. Mammal-mediated dispersal (Richardson and Young, 1977; Heinken, 1999), birds (Bailey and James, 1979), or snails (Boch et al, 2011) might also play a role in the distribution pattern observed in Quebec, or possibly the strong winds and winter storms common to the region. Högberg et al. (2002) suggested that transoceanic migration of the lichen *Letharia vulpina* (L.) Hue from western North America to Europe occurred via lightweight soredia. Another potential explanation is that sexual reproduction is more frequent than commonly believed

TABLE 3. Summary statistics for *Cladonia stellaris* and *C. mitis* from different succession fire stages in the *Parc National des Grands-Jardins*. Results derived from the bwa-mapping approach and filtered with *-r 0.75 --max-obs-het 0 --min-maf 0.05*. All positions (variant and fixed) are shown. Statistics include Num ind. (total average number of individuals genotyped at each locus), private sites (number of unique sites to each population), sites (total number of sites for each population), variant sites (number of sites across all populations that are variant), polymorphic sites (SNPs) (number of sites inside each population that are variant), PPS% (percentage of polymorphic sites), and π (mean nucleotide diversity).

bwa-mapping **# All positions (variant and fixed)**								
Successional fire stage	**Num Ind**	**Private**	**Sites**	**Variant**	**% Variant**	**Polymorphic**	**% PPS**	**π**
1999 (*C. mitis*)	4.66	1659	304609	5484	1.80	3022	0.99	0.0042
1991 (*C. stellaris*)	11.08	87	214427	3876	1.81	1884	0.88	0.0030
1940 (*C. stellaris*)	14.17	94	213265	3881	1.82	1904	0.89	0.0029
1921 (*C. stellaris*)	14.36	36	175750	3054	1.74	1501	0.85	0.0027
1864 (*C. stellaris*)	25.75	26	167828	2899	1.73	1511	0.90	0.0026

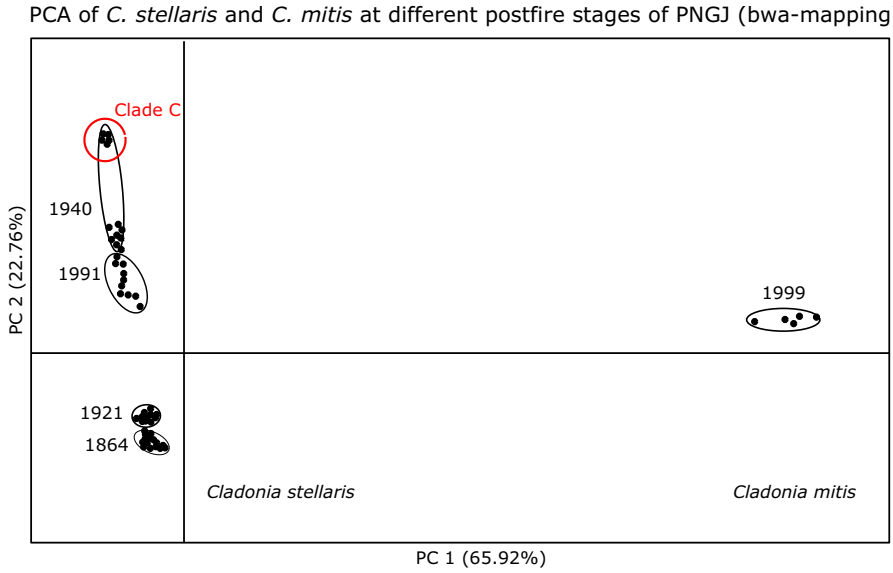

FIGURE 7. PCA of *Cladonia stellaris* and *C. mitis* from different succession fire stages in *Parc National des Grands-Jardins*. Results inferred using 7314 SNPs from the bwa-mapping approach. Popmap PNGJ species and fire (Appendix S1, Table S1).

in *C. stellaris* (Ahti, 1961). Fungal spores can disperse several hundred meters to kilometers (e.g., Heinken, 1999; Werth, 2010; Alors et al., 2017; Ronnås et al., 2017), which would explain the lack of spatial structure of the species and mixing of the haplotypes. We confirm the presence of apothecia (sexual structures) (Fig. 1C) in less than 10% of the individuals examined here. Some fungal groups with a supposedly asexual lifestyle indeed have the ability to undergo cryptic sexual reproduction (Kück and Pöggeler, 2009; Ene and Bennett, 2014).

Throughout the Quebec region, we found four supported evolutionary lineages of *C. stellaris* (clades A, B, C, and D) (Fig. 4, Appendix S3). Clade A is present all over the study region, but it is mainly distributed toward the North (Appendix S8). Clade B is exclusively distributed in southern Quebec (Appendix S8) and exhibited the greater values of genetic diversity (Table 2) and less co-ancestry (Fig. 6). It seems that southern Quebec populations harbor more genetic diversity than those from the North. On the other hand, clade C was composed of five samples in bwa-mapping (Fig. 3) but split into two independent clades with bowtie2-mapping (Appendix S3). The five individuals were collected in PNGJ, in the 1940 fire site. The remaining samples from the 1940 fire site were not included in clade C. This clade presented the lowest values of genetic diversity for both approaches with great differences in SNPs number (Table 2) likely due to the different approaches.

Regarding the genetic isolation among lineages, the number of variant sites was always higher than the number of SNPs (Table 2), meaning higher genetic diversity among lineages than within them (Allen et al., 2018). Here, we considered *Fst* values over 0.25 as having pronounced levels of genetic differentiation (Freeland et al., 2011). We did not find high genetic differentiation among lineages, with the 1940 fire site (clade C) being the most different (*Fst* = 0.22) (Appendix S1, Table S8). The absence of genetic differentiation might imply elevated levels of gene flow between lineages of *C. stellaris*. Recently, studies based on SNPs data sets or microsatellites assessed the rates of gene flow in lichens. Allen et al. (2018) found low rates of gene flow (*Fst* values 0.317–0.730) among southern Appalachian populations of the species *Cetradonia linearis* (Evans) J.C. Wei & Ahti. By contrast, in the Mediterranean Basin, Alors et al. (2017) detected high connectivity (*Fst* < 0.016) among populations of the strictly sexual *Parmelina carporrhizans* (Taylor) Poelt & Vězda.

Lack of correlation between genetic diversity and fire events

Reindeer lichens colonize burned sites around 20 years after a fire. *Cladonia mitis* arrives first, while *C. stellaris* does not usually colonize the site until 30 years after a fire (e.g., Ahti, 1959; Webb, 1998; Girard et al., 2017). Then, *C. stellaris* becomes the dominant species. Here, we first confirmed the differences at species level (between *C. mitis* and *C. stellaris*) (Appendix S6) and estimated genetic variation within each species (Appendix S1, Table S9). Our data indicated greater diversity in *C. mitis* than in *C. stellaris*, as some authors have already suggested. Athukorala et al. (2016) pointed out the intraspecific variation in the ITS rDNA of all reindeer lichens (except for *C. stellaris*). Other studies focused exclusively on *C. mitis* (as *C. arbuscula* s.l.) to highlight the elevated genetic variation in the species (Piercey-Normore et al., 2010; Athukorala et al., 2016).

Plotting the genetic data in the PCA (Fig. 7) and calculating *Fst* values (Appendix S1, Table S11), we verified that differences between species were higher (*Fst* > 0.75) than inside *C. stellaris* (*Fst* < 0.07). In contrast, there was little differentiation within *C. stellaris* throughout all the stages of the postfire succession.

To assess genetic diversity along the successional postfire chronosequence, samples of *C. mitis* from the most recent site (fire site 1999) and *C. stellaris* from the remaining sites (1991, 1940, 1921, and 1864) were included in the comparison. *Cladonia mitis* exhibited more genetic variation (SNPs and private sites), as our previous analysis reported. In *C. stellaris*, we found very similar values of genetic diversity (SNP number 1884, 1904, 1501, and 1511) in the four fire events (1991, 1940, 1921, and 1864), respectively (Table 3). Some studies have suggested that lichens from fire-disturbed areas have a significantly lower genetic diversity (Werth et al., 2006; Singh et al., 2015). Zouaoui et al. (2014) found that time since the last fire increased the probability that thallus fragments successfully reached different sites, thus, older areas were supposed to have higher rates of colonization and consequently, higher levels of genetic diversity. However, this was not observed within PNGJ. Our results agree with Gjerde et al. (2012), who used microsatellite markers in *Lobaria pulmonaria*, to show no significant genetic differences between young (55–120 yr) and old forest (140–200 yr) stands. Probably genetic diversity in recently burned areas is not lower than in mature LWs, because remnants of the prefire condition survived and mixed with newly arrived immigrant fragments augmenting the genetic diversity.

Adittionally, sexually-reproducing lichens species are supposed to exhibit higher genetic diversity than their asexual

counterparts (e.g., Seymour et al., 2005; Werth, 2010; Grewe et al., 2018). Populations of *C. stellaris* from PNGJ exhibited high levels of genetic diversity. However, sexual structures (apothecia, Fig. 1C) were rarely found (<10% of the individuals collected). These odd results may be explained by LDD of thallus fragments (Werth et al., 2006). It means that the colonization process would be governed mainly by LDD with mixing of genoytpes. Another explanation would be, as said above, cryptic sexuality in *C. stellaris*. There is some evidence for the occurrence of cryptic sex in filamentous fungi in which sexual reproduction had not been previously reported (e.g., Kück and Pöggeler, 2009). Recently, Del-Prado et al. (2016) suggested that cryptic sexuality may be contributing to the genetic diversity in the *Parmotrema reticulatum* complex, a fungal group traditionally considered as strictly asexual. A similar situation might be happening in *C. stellaris*, which would explain the high levels of genetic diversity in spite of the shortage of apothecia.

CONCLUSIONS

The study of *C. stellaris*, the most emblematic member of the LWs, showed that populations from southern Quebec are not genetically different from those of northern LWs. We identified four supported lineages with little geographic structure. The results point to constant migration between populations within the region. Whether LDD occurs via sexual spores or asexual propagules via biotic or abiotic vectors remains unknown. The finding of abundant apothecia and high levels of genetic diversity may suggest commonplace sexual reproduction—more common than previously reported.

At the landscape scale (PNGJ), we found no differences in values of genetic diversity along the four stages (1991, 1940, 1921, and 1864) of the postfire succession. We hypothesized that thallus fragments survive after a fire event, mixing with newcomer fragments and increasing diversity. The very low local genetic uniformity in PNGJ suggests recurring LDD of thallus fragments or cryptic sexual reproduction in *C. stellaris*.

To further elucidate the phylogeography of the species and the effect of fire on genetic diversity, higher sampling effort in northern Quebec and across Canada is needed. Thus, it would be possible to determine whether the number of cryptic lineages within *C. stellaris*. A detailed morphological examination of new samples would clarify the incidence of apothecia and allow estimation of the occurrence of sexual reproduction. In addition, to gain an understanding of clonality of this species, it would be advisable to expand sampling by using a grid design and substantially increasing the number of lichens sampled.

ACKNOWLEDGMENTS

We would like to thank the *Plateforme Analyse Génomique* and *Plateforme Bio-informatique* from the *Institut de Biologie Intégrative et des Systèmes* (Laval University, Quebec) for sequencing and for advice during the analysis of data. All manipulation of sequence reads was implemented on the UNIX server of Laval University. We thank the authorities of the *Parc National des Grands-Jardins* for giving us the permission to collect samples. We are also grateful to Catherine Chagnon for gathering samples northern Quebec, Philip Bell-Doyon for his help editing the maps, and Kim Damboise for pictures of apothecia. Comments of two reviewers and the editor have really improved the manuscript. MAG would like to thank the Science Visiting Scholarships from the Field Museum of Chicago for the six weeks stay at the Museum. This research was conducted with financial support from the Spanish *Fundación Séneca-Agencia de Ciencia y Tecnología de la Región de Murcia* (project 20369/PD/17) and the CRNSG- RGPIN/05967-2016 and Fondation canadienne pour l'innovation, project 36781.

AUTHOR CONTRIBUTIONS

M.A.G. planned the study, conducted field work, and performed and analyzed genomic data. F.G. provided guidance in analyzing genomic data and helped with analytical tools. S.P. planned fieldwork, provided research context, natural history, and geographic data on the species and the ecosystem. J.C.V. conceived, designed, and planned the study. All authors contributed to the writing of the manuscript.

DATA AVAILABILITY

Raw sequences data were deposited in the NCBI Sequence Read Archive (SRA) with accession numbers SAMN13450524–SAMN13450653 (BioProject ID PRJNA593044).

SUPPORTING INFORMATION

Additional Supporting Information may be found online in the supporting information tab for this article.

APPENDIX S1, TABLE S1. *Cladonia stellaris* and *C. mitis* samples collected in the Quebec province. The following information is provided for each individual: voucher (sample), species name, bioclimatic domain, location in Quebec, collection sites, and coordinates (latitude and longitude). Classification of samples for each population map (popmap) is also indicated (popmap denovo test, popmap PNGJ species, popmap PNGJ species and fire, popmap RAxML bowtie2-mapping, popmap RAxML bwa-mapping). Finally, classification of samples derived by the co-ancestry analysis is presented (fineRAD results bowtie2-mapping and fineRAD results bwa-mapping).

APPENDIX S1, TABLE S2. Reads information after demultiplexing with *process-radtags* (Stacks). Total number of reads, rad tags, low quality and retained reads are provided for each sample. A bar graph as well as the percentage of retained reads are shown.

APPENDIX S1, TABLE S3. Results derived from alignments with bowtie2 and bwa. All reads retained from *process-radtags* were included in the alignments (read_no). Those successfully mapped to the reference are shown (mapped_no) and the percentage of mapping calculated (per_mapped). A curve graph to compare results from the two software is also provided.

APPENDIX S1, TABLE S4. The *gstacks* results for the four approaches (bowtie2-mapping, bwa-mapping, bowtie2-denovo, bwa-denovo). Number of loci (n_loci), number of forward reads used to run *gstacks* (n_used_fw_reads), coverage (mean_cov and mean_cov_ns) and number of genotypes (n_gts) are shown. Two curve graphs are also incorporated to compare number of loci and coverage among approaches.

APPENDIX S1, TABLE S5. Summary population statistics for each individual with the four approaches (bowtie2-mapping, bwa-mapping, bowtie2-denovo, bwa-denovo). Statistics include private sites (alleles unique to each individual), sites (total number of sites), variant sites (variant sites across all individuals) and polymorphic sites (SNPs) (variant sites inside each individual). A curve graph is incorporated to compare number of variant sites among approaches.

APPENDIX S1, TABLE S6. Percentage of missing SNPs per sample inferred with the Adegenet package for the bowtie2-mapping data set (275 SNPs) and bwa-mapping data set (1450 SNPs). A curve graph is incorporated to compare results between approaches.

APPENDIX S1, TABLE S7. Summary population statistics for the phylogenetic clades of *Cladonia stellaris* in Quebec. Results derived from the bowtie2-mapping approach and filtered with *-r 0.75 --max-obs-het 0 --min-maf 0.05*. All positions (variant and fixed) are shown. Statistics include Num ind. (total average number of individuals genotyped at each locus), private sites (number of unique sites to each population), sites (total number of sites for each population), variant sites (number of sites across all populations that are variant), % variant (percentage of variant sites), polymorphic sites (SNPs) (number of sites inside each population that are variant), PPL% (percentage of polymorphic sites), and π (mean nucleotide diversity).

APPENDIX S1, TABLE S8. Pairwise *Fst* values among phylogenetic clades of *Cladonia stellaris*. Values above the diagonal correspond to bowtie2-mapping approach and below the diagonal to bwa-mapping. A curve graph is also incorporated to compare pairwise *Fst* values between approaches.

APPENDIX S1, TABLE S9. Summary population statistics for two species of *Cladonia*. *Cladonia stellaris* and *C. mitis* from *Parc National des Grands-Jardins*. Filtered with *-r 0.75 --max-obs-het 0 --min-maf 0.05*. All positions (variant and fixed) are shown. Statistics include Num ind. (total average number of individuals genotyped at each locus), private sites (number of unique sites to each population), sites (total number of sites for each population), variant sites (number of sites across all populations that are variant), polymorphic sites (SNPs) (number of sites inside each population that are variant), PPL% (percentage of polymorphic sites) and π (mean nucleotide diversity). (A) Results derived from the bwa-mapping approach. (B) Results derived from the bowtie2-mapping approach.

APPENDIX S1, TABLE S10. Summary statistics for *Cladonia stellaris* and *C. mitis* from different succession fire stages in the *Parc National des Grands-Jardins*. Results derived from the bowtie2-mapping approach and filtered with *-r 0.75 --max-obs-het 0 --min-maf 0.05*. All positions (variant and fixed) are shown. Statistics include "Num ind." (total average number of individuals genotyped at each locus), private sites (number of unique sites to each population), sites (total number of sites for each population), variant sites (number of sites across all populations that are variant), polymorphic sites (SNPs) (number of sites inside each population that are variant), PPL% (percentage of polymorphic sites), and π (mean nucleotide diversity).

APPENDIX S1, TABLE S11. Pairwise *Fst* values among *Cladonia stellaris* and *C. mitis* from different succession fire stages in *Parc National des Grands-Jardins*. Values below the diagonal correspond to bwa-mapping approach and above the diagonal to bowtie2-mapping.

APPENDIX S2. Scripts.

APPENDIX S3. Maximum likelihood phylogenetic trees inferred from *Cladonia stellaris* genotyping-by-sequencing (GBS) data. Trees resulted from 171 unlinked SNPs data set from bowtie2-mapping approach, midpoint rooted. Well-supported branches (Bootstrap values >70) are marked with a start. The same colors as in Fig. 4 were used to represent each clade (purple to clade A, orange to clade B, red to clade C, and orange to clade D).

APPENDIX S4. PCA of *Cladonia stellaris* in Quebec using 275 SNPs from the bowtie2-mapping approach. Letters correspond with maximum likelihood phylogenetic clades (Appendix S3).

APPENDIX S5. Clustered fineRADstructure co-ancestry matrix of *Cladonia stellaris* in Quebec estimated from 171 unlinked SNPs from the bowtie2-mapping approach. The heatmap shows pairwise co-ancestry between individuals, with blue representing the highest level, red and orange indicating intermediate levels, and yellow representing the lowest levels of shared co-ancestry. The names of clades follow those of the maximum likelihood tree (Appendix S3).

APPENDIX S6. PCA of *Cladonia stellaris* and *C. mitis* in *Parc National des Grands-Jardins* using (A) 5329 SNPs data set from bwa-mapping approach, and (B) 987 SNPs data set from the bowtie2-mapping approach. Popmap PNGJ species (Appendix S1, Table S1). Pairwise *Fst* values are included.

APPENDIX S7. PCA of *Cladonia stellaris* and *C. mitis* from different succession fire stages in *Parc National des Grands-Jardins*. Results inferred using 1203 SNPs from the bowtie2-mapping approach. Popmap PNGJ species and fire (Appendix S1, Table S1).

APPENDIX S8. Map of the geographical distribution of samples of *Cladonia stellaris* according to their genetical position in the phylogenetic tree is inferred by bwa-mapping (Fig. 4). Clades A (purple square), B (orange triangle), C (red circle), D (green circle), and E (black circle). The different ecosystems are highlighted.

LITERATURE CITED

Ahti, T. 1959. Studies on the caribou lichen stands of Newfoundland. *Annales Botanici Societatis Zoologicae Botanicae Fennicae 'Vanamo'* 30: 1–44.

Ahti, T. 1961. Taxonomic Studies on Reindeer Lichens (*Cladonia*, Subgenus *Cladina*). Suomalaisen Kirjallisuuden Kirjapaino, Helsinki, Finland.

Allen, J. L., S. K. McKenzie, R. S. Sleith, and S. E. Alter. 2018. First genome-wide analysis of the endangered, endemic lichen *Cetradonia linearis* reveals isolation by distance and strong population structure. *American Journal of Botany* 105: 1556–1567.

Alors, D., F. D. Grande, P. Cubas, A. Crespo, I. Schmitt, M. C. Molina, and P. K. Divakar. 2017. Panmixia and dispersal from the Mediterranean Basin to Macaronesian Islands of a macrolichen species. *Scientific Reports* 7: 1–9.

Anderson, E., and E. D. Rudolph. 1956. An analysis of variation in a variable population of *Cladonia*. *Evolution* 10: 147–156.

Andrews, S. 2010. fastqc: a quality control tool for high throughput sequence data (Version 0.11.3). Website: http://www.bioinformatics.babraham.ac.uk/projects/fastqc.

Armaleo, D., O. Muller, F. Lutzoni, O. S. Andresson, G. Blanc, H. B. Bode, F. R. Collart, et al. 2019. The lichen symbiosis re-viewed through the genomes of *Cladonia grayi* and its algal partner *Asterochloris glomerata*. *BMC Genomics* 20: 605.

Asselin, H., and S. Payette. 2005. Late Holocene opening of the forest tundra landscape in northern Quebec, Canada. *Global Ecology and Biogeography* 14: 307–313.

Athukorala, S. N. P., J. Doering, and M. D. Piercey-Normore. 2016. Morphological and genetic polymorphism in two North American reindeer lichens: *Cladonia arbuscula* and *C. rangiferina*. *Ceylon Journal of Science (Biological Sciences)* 44: 55–65.

Athukorala, S. N. P., R. Pino-Bodas, S. Stenroos, T. Ahti, and M. D. Piercey-Normore. 2016. Phylogenetic relationships among reindeer lichens of North America. *Lichenologist* 48: 209–227.

Auclair, A. N. D., and A. N. Rencz. 1982. Concentration, mass, and distribution of nutrients in a subarctic *Picea mariana–Cladonia alpestris* ecosystem. *Canadian Journal of Forest Research* 12: 947–968.

Bailey, R., and P. James. 1979. Birds and dispersal of lichen propagules. *Lichenologist* 11: 105–106.

Bergeron, Y., and M. Dubuc. 1989. Succession in the southern part of the Canadian boreal forest. *Vegetation* 79: 51–63.

Bergeron, Y., S. Gauthier, V. Kafka, P. Lefort, and D. Lesieur. 2001. Natural fire frequency for the eastern Canadian boreal forest: consequences for sustainable forestry. *Canadian Journal of Forest Research* 31: 384–391.

Bergerud, A. T. 1971. Abundance of forage on the winter range of newfoundland caribou. *The Canadian Field Naturalist* 85: 39–52.

Boch, S., D. Prati, S. Werth, J. Rüetschi, and M. Fischer. 2011. Lichen endozoochory by snails. *PLoS One* 6: 2–6.

Bowler, P. A., and P. W. Rundel. 1975. Reproductive strategies in lichens. *Botanical Journal of the Linnean Society* 70: 325–340.

Brodo, I. M., S. D. Sharnoff, and S. Sharnoff. 2001. Lichen of North America. New Haven and London: Yale University Press.

Coxson, D. S., and J. Marsh. 2001. Lichen chronosequences (postfire and postharvest) in lodgepole pine (*Pinus contorta*) forests of northern interior British Columbia. *Canadian Journal of Botany* 79: 1449–1464.

Degtjarenko, P., T. Tõrra, T. Mandel, L. Marmor, A. Saag, C. Scheidegger, and T. Randlane. 2018. Unconstrained gene flow between populations of a widespread epiphytic lichen *Usnea subfloridana* (Parmeliaceae, Ascomycota) in Estonia. *Fungal Biology* 122: 731–737.

DeGrandpré, L., D. Gagnon, and Y. Bergeron. 1993. Changes in the understory of Canadian boreal forest after fire. *Journal of Vegetable Science* 4: 803–810.

Del-Prado, R., P. K. Divakar, H. T. Lumbsch, and A. Crespo. 2016. Hidden genetic diversity in an asexually reproducing lichen forming fungal group. *PLoS One* 11: 1–18.

Ene, I., and R. Bennett. 2014. The cryptic sexual strategies of human fungal pathogens. *Nature Reviews Microbiology* 12: 239–251.

Freeland, J. R., S. D. Petersen, and H. Kirk. 2011. Molecular Ecology (2nd Edition). John Wiley and Sons, West Sussex, United Kingdom.

Gauslaa, Y. 1997. Population structure of the epiphytic lichen *Usnea longissima* in a boreal *Picea abies* canopy. *Lichenologist* 29: 455–469.

Gauthier, L., R. Nault, and M. Crête. 1989. Variations saisonnières du régime alimentaire des caribous du troupeau de la rivière George, Québec nordique. *Le Naturaliste canadien* 116: 101–112.

Girard, F., S. Payette, and A. Delwaide. 2017. Patterns of early postfire succession of alpine, subalpine and lichen-woodland vegetation: 21 years of monitoring from permanent plots. *Forests* 8: 1–14.

Gjerde, I., H. H. Blom, L. Lindblom, M. Sætersdal, and F. H. Schei. 2012. Community assembly in epiphytic lichens in early stages of colonization. *Ecology* 93: 749–759.

Grewe, F., J. P. Huang, S. D. Leavitt, and H. T. Lumbsch. 2017. Reference-based RADseq resolves robust relationships among closely related species of lichen-forming fungi using metagenomic DNA. *Scientific Reports* 7: 1–11.

Grewe, F., E. Lagostina, H. Wu, C. Printzen, and H. T. Lumbsch. 2018. Population genomic analyses of RAD sequences resolves the phylogenetic relationship of the lichen-forming fungal species *Usnea antarctica* and *Usnea aurantiacoatra*. *MycoKeys* 43: 91–113.

Heinken, T. 1999. Dispersal patterns of terricolous lichens by thallus fragments. *Lichenologist* 31: 603–612.

Héon, J., D. Arseneault, and M. A. Parisien. 2014. Resistance of the boreal forest to high burn rates. *Proceedings of the National Academy of Science of the United States of America* 38: 13888–13893.

Högberg, N., S. Kroken, G. Thor, and J. W. Taylor. 2002. Reproductive mode and genetic variation suggest a North American origin of European *Letharia vulpina*. *Molecular Ecology* 11: 1191–1196.

Hustich, I. 1957. On the phytogeography of the subarctic Hudson Bay lowland. *Acta Geographica* 16: 1–48.

Jasinski, J. and S. Payette. 2005. The creation of alternative stable states in the southern boreal forest, Quebec, Canada. *Ecological Monographs* 75: 561–583.

Johnson, E. A., and K. Miyanishi. 1999. Subarctic lichen woodlands. *In* R. C. Anderson, J. S. Fralish, and J. M. Baskin [eds.], Savannas, Barrens, and Rock Outcrop Plant Communities of North America, 421–436.Cambridge University Press, New York, USA.

Jombart, T., Z. N. Kamvar, R. Lustrik,C. Collins, M. P. Beugin, B. Knaus, and F. Calboli. 2016. adegenet: Exploratory analysis of genetic and genomic data (version 2.0.1). Computer program and documentation distributed by the author. Website: https://cran.r-project.org/web/packages/adegenet/index.html.

Kenkel, N. C., D. J. Walker, P. R. Watson, R. T. Caners, and R. A. Lastra. 1997. Vegetation dynamics in boreal forest ecosystems. *Coenoses* 12: 97–108.

Kershaw, K. A. 1978. The role of lichens in boreal tundra transition areas. *The Bryologist* 81: 294–306.

Kershaw, K. A., and W. R. Rouse. 1976. The impact of fire on forest and tundra ecosystems. *Final Report* 1975. Arctic Land Use Research. Program Report 75-76-63.

Kück, U., and S. Pöggeler. 2009. Cryptic sex in fungi. *Fungal Biology Reviews* 23: 86–90.

Lafleur, B., S. Zouaoui, N. J. Fenton, P. Drapeau, and Y. Bergeron. 2016. Short-term response of Cladonia lichen communities to logging and fire in boreal forests. *Forest Ecology and Management* 372: 44–52.

Langmead, B., and S. L. Salzberg. 2012. Fast gapped-read alignment with Bowtie 2. *Nature Methods* 9: 357–359.

Li, H. 2013. Aligning sequence reads, clone sequences and assembly contigs with BWA-MEM. Computer program and documentation distributed by the author. Website: https://arxiv.org/abs/1303.3997.

Li, H., and R. Durbin. 2009. Fast and accurate short read alignment with Burrows-Wheeler Transform. *Bioinformatics* 25: 1754–1760.

Maikawa, E., and K. A. Kershaw. 1976. Studies on lichen dominated systems. XIX. The postfire Québec's closed-crown forest zone. *American Journal of Plant Science* 4: 749–765.

Malinsky, M., E. Trucchi, D. J. Lawson, and D. Falush. 2018. RADpainter and fineRADstructure: Population inference from RADseq data. *Molecular Biology and Evolution* 35: 1284–1290.

Mascher, M., S. Wu, P. St. Amand, N. Stein, and J. Poland. 2013. Application of Genotyping-by-Sequencing on Semiconductor Sequencing Platforms: A Comparison of Genetic and Reference-Based Marker Ordering in Barley. *PLoS One* 8: e76925.

Morneau, C., and S. Payette. 1989. Postfire lichen-spruce woodland recovery at the limit of the boreal forest in northern Quebec. *Canadian Journal of Botany* 67: 2770–2782.

Pan, J., B. Wang, Z. Y. Pei, and J. Gao. 2015. Optimization of the genotyping-by-sequencing strategy for population genomic analysis in conifers. *Molecular Ecology* 15: 771–722.

Paris, J. R., J. R. Stevens, and J. M. Catchen. 2017. Lost in parameter space: A road map for stacks. *Methods in Ecology and Evolution* 8: 1360–1373.

Park, S., S. Jang, S. Oh, J. A. Kim, and J. Hur. 2014. An easy, rapid, and cost-effective method for DNA extraction from various lichen taxa and specimens suitable for analysis of fungal and algal strains. *Mycobiology* 42: 311–320.

Payette, S. 1992. Fire as a controlling process in the North American boreal forest. *In* H. H. Shugart, R. Leemans, and G. B. Bonan [eds.], A Systems

Analysis of the Global Boreal Forest, 144–165.Cambridge University Press, Cambridge, United Kingdom.

Payette, S., N. Bhiry, A. Delwaide, and M. Simard. 2000. Origin of the lichen woodland at its southern range limit in eastern Canada: the catastrophic impact of insect defoliators and fire on the spruce–moss forest. *Canadian Journal of Forest Research* 30: 288–305.

Payette, S., and A. Delwaide. 2018. Tamm review: The North-American lichen woodland. *Forest Ecology and Management* 417: 167–183.

Payette, S., M. Fortin, and I. Gamache. 2001. The subarctic forest–tundra: the structure of a biome in a changing climate. *BioScience* 51: 709–718.

Payette, S., C. Morneau, L. Sirois, and M. Desponts. 1989. Recent fire history of the northern Quebec biomes. *Ecology* 70: 656–673.

Piercey-Normore, M. D., T. Ahti, and T. Goward. 2010. Phylogenetic and haplotype analyses of four segregates within *Cladonia arbuscula* s.l. *Botany* 88: 397–408.

Richardson, D. H. S., and C. M. Young. 1977. Lichens and Vertebrates. *In* M. R. D. Seaward [ed.], Lichen Ecology, 121–144.Academic Press, London, United Kingdom.

Rochette, N. C., and J. M. Catchen. 2017. Deriving genotypes from RAD- seq short-read data using Stacks. *Nature Protocols* 12: 2640–2659.

Rochette, N. C., A. G. Rivera-Colón, and J. M. Catchen. 2019. Stacks 2: Analytical methods for paired-end sequencing improve RADseq-based population genomics. *Molecular Ecology* 28: 4737–4754.

Ronnås, C., S. Werth, O. Ovaskainen, G. Várkonyi, C. Scheidegger, and T. Snäll. 2017. Discovery of long-distance gamete dispersal in a lichen-forming ascomycete. *The New phytologist* 216: 216–226.

Seymour, F. A., P. D. Crittenden, and P. S. Dyer. 2005. Sex in the extremes: lichen-forming fungi. *Mycologist* 19: 51–58.

Shaver, G. R., and F. S. Chapin. 1991. Production: biomass relationships and element cycling in contrasting arctic vegetation types. *Ecological Monographs* 61: 1–31.

Simard, M., and S. Payette. 2001. Black spruce decline triggered by spruce budworm at the southern limit of lichen woodland in eastern Canada. *Canadian Journal of Forest Research* 31: 2160–2172.

Singh, G., F. Dal Grande, S. Werth, and C. Scheidegger. 2015. Long-term consequences of disturbances on reproductive strategies of the rare epiphytic lichen *Lobaria pulmonaria*: Clonality a gift and a curse. *FEMS Microbiology Ecology* 91: 1–11.

Spalink, D., R. MacKay, and K. J. Sytsma. 2019. Phylogeography, population genetics, and distribution modeling reveal vulnerability of *Scirpus longii* (Cyperaceae) and the Atlantic Coastal Plain flora to climate change. *Molecular Ecology* 28: 2046–2061.

Stamatakis, A. 2014. RAxML version 8: a tool for phylogenetic analysis and post-analysis of large phylgogenies. *Bioinformatics* 30: 1312–1313.

Stenroos, S., R. Pino-Bodas, J. Hyvönen, H. T. Lumbsch, and T. Ahti. 2018. Phylogeny of the family Cladoniaceae (Lecanoromycetes, Ascomycota) based on sequences of multiple loci. *Cladistics* 35: i–ii, 351–460.

Svihus, B., and Ø. Holand. 2000. Lichen polysaccharides and their relation to reindeer/caribou nutrition. *Journal of Range Management* 53: 642–648.

Vainio, E. A. 1897. Monographia *Cladoniarum universalis*. 3. *Acta Societatis pro Fauna et Flora Fennica* 14: 1–268.

Vézeau, C., and S. Payette. 2016. Gap expansion in old-growth subarctic forests: The climate–pathogen connection. *New Phytology* 212: 1044–1056.

Walser, J. C., R. Holderegger, F. Gugerli, S. E. Hoebee, and C. Scheidegger. 2005. Microsatellites reveal regional population differentiation and isolation in *Lobaria pulmonaria*, an epiphytic lichen. *Molecular Ecology* 14: 457–467.

Webb, E. T. 1998. Survival, persistence, and regeneration of the reindeer lichens, *Cladina stellaris*, *C. rangiferina*, and *C. mitis* following clear cut logging and forest fire in northwestern Ontario. *Rangifer* 10: 19–21.

Werth, S. 2010. Population genetics of lichen-forming fungi—A review. *Lichenologist* 42: 499–519.

Werth, S., F. Gugerli, R. Holderegger, H. H. Wagner, D. Csencsics, and C. Scheidegger. 2007. Landscape-level gene flow in *Lobaria pulmonaria*, an epiphytic lichen. *Molecular Ecology* 16: 2807–2815.

Werth, S., H. H. Wagner, R. Holderegger, J. M. Kalwij, and C. Scheidegger. 2006. Effect of disturbances on the genetic diversity of an old-forest associated lichen. *Molecular Ecology* 15: 911–921.

Yarranton, G. A. 1975. Population growth in *Cladonia stellaris* (Opiz.) Pouz. and Vezda. *New Phytologist* 75: 99–110.

Zouaoui, S., C. Boudreault, P. Drapeau, and Y. Bergeron. 2014. Influence of time since fire and micro-habitat availability on terricolous lichen communities in Black Spruce (*Picea mariana*) boreal forests. *Forests* 5: 2793–2809.